Machine learning approach for prediction of hepatic enhancement during the hepatobiliary phase of Gd-EOB DTPA-enhanced MRI.

Ji Su Ko
Department of Radiology, Hallym University College of Medicine, Kangnam Sacred Heart Hospital
Jieun Byun (sueno54@naver.com)
Department of Radiology, Hallym University College of Medicine, Kangnam Sacred Heart Hospital
Seongkeun Park
Machine Intelligence Laboratory, Department of Smart Automobile, Soonchunhyang University
Ji Young Woo
Department of Radiology, Hallym University College of Medicine, Kangnam Sacred Heart Hospital

Research Article

Keywords: chronic liver disease, cirrhosis, magnetic resonance imaging (MRI), Gd-EOB-DTPA, Child-Pugh score (CPS)

Posted Date: March 11th, 2021

DOI: https://doi.org/10.21203/rs.3.rs-274189/v1

Abstract

We retrospectively assessed 214 patients with chronic liver disease or liver cirrhosis who underwent magnetic resonance imaging (MRI) enhanced with gadolinium ethoxybenzyl diethylenetriamine pentaacetic acid (Gd-EOB-DTPA) from August 2016 to May 2020 to evaluate the relationship between biochemical results that reflect liver function and hepatic enhancement. With the information gained we employed a machine learning approach with the K-Nearest Neighbor (KNN) algorithm to develop a predictive model for determining insufficient hepatic enhancement during the hepatobiliary phase (HBP) in Gd-EOB-DTPA-enhanced MRI. Using both quantitative and qualitative assessments, the total bilirubin (TB), albumin (Alb), prothrombin time-international normalized ratio, platelet, Child-Pugh score (CPS), and Model for End-stage Liver Disease Sodium (MELD-Na) score were related to decreased hepatic enhancement. In a multivariate analysis, TB and Alb were associated with insufficient enhancement ($p < 0.001$). The predictive model showed that a combination of a variety of biochemical parameters had better performance (accuracy = 82.8%, area under the curve (AUC) = 0.861) in predicting insufficient enhancement than either the CPS (accuracy = 79.5%, AUC = 0.845) or the MELD-Na score (accuracy = 80.8%, AUC = 0.821). By using a machine-learning-based predictive model with the KNN algorithm, radiologists can predict insufficient hepatic enhancement during HBP in advance and adjust each patient's individually optimized MRI protocol.

Introduction

The liver-specific contrast agent gadolinium ethoxybenzyl diethylenetriamine pentaacetic acid (Gd-EOB-DTPA) has gained attention in recent years and has been included in a guideline on the management of hepatocellular carcinoma [1]. This contrast medium allows for the assessment of tissue perfusion during hepatocyte-specific imaging. It helps in the detection and differentiation of focal liver lesions through a comparative evaluation between the hepatobiliary phase (HBP) and other vascular phases [2,3].

In patients with normal liver function, 50% of Gd-EOB-DTPA is uptaken by the hepatocyte through the organic anion-transporting polypeptides membrane transporter, and then secreted into the bile duct by an exporter transporter such as multidrug resistance-associated protein 2. The other half of the Gd-EOB-DTPA passes through the vessel after extracellular space distribution and is excreted through the kidney [4–6]. As a result, in patients with impaired liver function, such as liver cirrhosis patients, the number of functioning hepatocytes decreases, resulting in a decrease in hepatocyte uptake of Gd-EOB-DTPA [7–9]. Insufficient enhancement of liver parenchyma has been reported to reduce diagnostic accuracy [7,10]. Therefore, it would be important to predict whether there will be insufficient enhancement before taking magnetic resonance imaging (MRI). There have been studies to predict insufficient enhancement during the HBP using the Child-Pugh score (CPS), the Model for End-stage Liver Disease (MELD) score, and a combination of other biochemical parameters [9,11]. However, research conducted in conjunction with machine learning has not yet been reported to the best of our knowledge.

The purpose of this study is to evaluate the relationship between a variety of biochemical results reflecting liver function and hepatic enhancement and develop a predictive model for determining insufficient hepatic enhancement during HBP in Gd-EOB-DTPA-enhanced MRI using a machine learning approach with the K-Nearest Neighbor (KNN) algorithm.

Materials And Methods

Patients

This retrospective study was conducted with the approval of the institutional review board at Kangnam Sacred Heart Hospital (Seoul, Korea), which waived requirements for written informed consent due to the retrospective nature of the study.
And all research was conducted following relevant guidelines and regulations.

We reviewed the records of 280 patients who were diagnosed with chronic liver disease or liver cirrhosis based on physical findings, biochemical tests, and radiological imaging features and underwent Gd-EOB-DTPA-enhanced MRI from August 2016 to May 2020.
Among them, 66 were excluded from this study because of the following criteria: 1) blood test results within 2 weeks were unavailable (n = 52); 2) there was infiltrative hepatocellular carcinoma (HCC) (n = 3); 3) there was chronic renal disease (n = 11). After eliminating the 66 patients, the remaining 214 patients (154 males and 60 females) were included in the study. The clinical and demographic characteristics of the study population, such as age, sex, and etiology of chronic liver disease were collected from electronic medical records.

MRI techniques

All MRI examinations were performed with two clinical 3T MRI systems (Magnetom Skyra; Siemens Healthcare, Erlangen, Germany, and Magnetom Vida; Siemens Healthcare, Erlangen, Germany). A combination of body and spine coil elements was used for signal acquisition, with patients holding their breath in the supine position. The HBP images were obtained 20 min after administration of Gd-EOB-DTPA (Primovist, Bayer Healthcare, Berlin, Germany).

The parameters of the HBP sequence were: repetition time (TR), 4.2 ms; echo time (TE), 1.2 ms; flip angle (FA), 15’; matrix size, 256 · 187; field of view (FOV), 308 · 380 mm^2; slice thickness, 3 mm; acquisition time, 15 s. Gadoxetic acid (0.025 mmoL/kg body weight) was administered via bolus injection (flow rate: 1 mL/s, flushed with 20 mL normal saline).

Image analysis

Analysis of MRI was retrospectively performed by three radiologists (WJY and BJ with > 10 years and KJS with 2 years of experience in interpretation of Gd-EOB-DTPA-enhanced MRI) who were kept unaware of related clinical information.

For quantitative analysis, regions of interest (ROI) analyses were performed. We drew 5–15 mm ROIs in diameter on the largest transversal slice of the liver of the HBP images, avoiding blood vessels, focal liver lesions, and artifacts. One ROI was placed in the middle of the right main branch of the portal vein and four ROIs were placed in the right lobe (anterior and posterior segments), and left lobe (medial and lateral segments). The liver-to-portal vein signal intensity ratio (LPR) was calculated by dividing the mean value of the signal intensity (SI) of the four liver parenchyma ROI by the SI of the portal vein. For qualitative assessment, visual scoring for relative hepatic enhancement relative to the portal vein on HBP images as liver-to-portal vein contrast (LPVC) was made using the following 5-level grading scale: 1, hyperintense; 2, slightly hyperintense; 3, isointense; 4, slightly hypointense; 5, hypointense [12]. An LPVC score ≥ 3 was considered as an insufficient hepatic enhancement [11]. Visual analysis was performed on different days at a 2-week interval from a quantitative assessment of SI for reducing recall bias, and the three reviewers were blinded to each other’s ROI measurements.

Biochemical test and liver function test

A variety of blood serum biochemical tests at the time of performing MRI, including alanine aminotransferase (ALT), aspartate aminotransferase (AST), gamma-glutamyl transpeptidase (GGT), alkaline phosphatase (ALP), albumin (Alb), total bilirubin (TB), platelet count (PLT), prothrombin time-international normalized ratio (PT-INR), activated partial thromboplastin time (aPTT), sodium (Na), and creatinine (Cr) were recorded. CPS and MELD-Na scores were also calculated for assessing hepatic function. The CPS was calculated from five variables including TB, Alb, PT, ascites status, and degree of encephalopathy [13]. The equation for the MELD-Na score was MELD-Na = 11.2 × ln(INR) + 9.57 × ln(Cr, in milligrams per deciliter) + 3.78 × ln(TB, in milligrams per deciliter) + 6.43 − Na − [0.025 × (11.2 × ln(INR) + 9.57 × ln(Cr, in milligrams per deciliter) + 3.78 × ln(TB, in milligrams per deciliter) + 6.43) × (140 − Na)] + 140 [14].

Statistical analysis

Continuous variables were expressed as the mean with standard deviation or the median with interquartile range. Categorical variables were expressed as number or frequency. Data were compared with the Student's *t*-test, the nonparametric Mann–Whitney *U* test, or the Kruskal-Wallis test for continuous variables, and the Chi-squared test or the Fisher's exact test for categorical variables, as appropriate. Relationships between the visual assessment of hepatic enhancement and LPR and clinical factors were assessed using Pearson's correlation coefficient (r) and Spearman's rank correlation coefficient (ρ).

Interobserver agreement for quantitative and qualitative analysis of hepatic enhancement on HBP images among the three radiologists was evaluated with kappa statistics (κ) and the interobserver correlation coefficient (ICC). The categories of the κ values were defined as follows: poor, less than 0.00; slight, 0.00–0.20; fair, 0.21–0.40; moderate, 0.41–0.60; substantial, 0.61–0.80; and almost perfect, 0.81–0.99 [15].

We performed uni- and multivariate logistic regression analyses to determine associates of insufficient hepatic enhancement by including the parameters that showed a significant difference in the univariate analyses. Biochemical parameters were used as variables, and calculated values such as CPS and MELD-Na were excluded.

These statistical analyses were performed using SPSS (version 21.0; SPSS, Inc., Chicago, IL, USA). A p-value < 0.05 was considered statistically significant. The predictive model for insufficient liver enhancement was developed using Matlab 2018b with the Statistical Machine and Deep Learning toolboxes. The utility of the machine learning algorithm for the prediction of insufficient hepatic enhancement was tested by omitting one cross-validation to calculate sensitivity, specificity, accuracy, and area under the curve (AUC) for CPS, MELD-Na, and the combination of biochemical parameters.

The details of the building process of the machine learning model using the KNN algorithm are provided in the Supplementary Information.

Results

Patients and MRI measurements.

Table 1 summarizes the demographics, etiology of liver disease, and laboratory values of the 214 patients. These patients included 154 men (mean age, 61.45 ± 11.03 years) and 60 women (mean age, 67.32 ± 11.05 years).

Hepatitis B virus was the most common cause of chronic liver disease (79.8%). The mean LPR was 1.84. Among 214 patients, 76 patients (35.5%) were classified as LPVC grade 1, 75 (35.0%) as LPVC grade 2, 57 (26.6%) as LPVC grade 3, six patients (2.8%) as LPVC grade 4, and there were no patients classified as grade 5.

Table 1
Baseline characteristic of the study population

characteristic		total (n = 214)
Age, years*		63.10 ± 11.32
Sex†	male	154 (71.9)
	female	60 (28.0)
Etiology†	Hepatitis B	126 (58.9)
	Hepatitis C	28 (13.1)
	Alcoholic liver disease	49 (22.9)
	primary biliary cirrhosis	2 (0.9)
	others‡	9 (4.2)
CPC†	A	177 (82.7)
	B	34 (15.9)
	C	3 (1.4)
CPS		6 (5, 7)
MELD-Na		8.5 (7, 12)
TB, ng/mL		0.9 (0.6, 1.6)
Alb, ng/mL		3.8 (3.28, 4.3)
PT-INR		1.12 (1.05, 1.24)
aPTT, sec		33.1 (29.9, 34.53)
AST, IU/L		38 (29, 63.25)
ALT, IU/L		31.5 (21, 50.25)
ALP, IU/L		98 (78, 140.25)
GGT, IU/L		60 (33.75, 126.25)

Note. - Unless otherwise specified, data are median with interquartile range.

* Data are presented as a mean ± standard deviation

† Data are presented as number (%) of patients

‡Including nonalcoholic steatohepatitis, autoimmune hepatitis, and cryptogenic liver disease.

CPC = Child-Pugh class, CPS = Child-Pugh score, MELD-Na = Model for End-stage Liver Disease and sodium, TB = total bilirubin, Alb = albumin, PT-INR = prothrombin time-international normalized ratio, aPTT = activated partial thromboplastin time, AST = aspartate aminotransferase, ALT = alanine aminotransferase, ALP = alkaline phosphatase, GGT = gamma-glutamyl transpeptidase, Cr = creatinine, Na = sodium, PLT = platelet, LPR = liver-to-portal vein signal intensity ratio, LPVC = liver-to-portal vein contrast

characteristic		total (n = 214)
Cr, mg/dL		0.8 (0.67, 0.96)
Na, mEq/L		138 (136, 140)
PLT, ×1000/uL		127.5 (80.75, 196.5)
LPVC†	1	76 (35.5)
	2	75 (35)
	3	57 (26.6)
	4	6 (2.8)
	5	0 (0)
Note. - Unless otherwise specified, data are median with interquartile range.		
* Data are presented as a mean ± standard deviation		
† Data are presented as number (%) of patients		
‡Including nonalcoholic steatohepatitis, autoimmune hepatitis, and cryptogenic liver disease.		
CPC = Child-Pugh class, CPS = Child-Pugh score, MELD-Na = Model for End-stage Liver Disease and sodium, TB = total bilirubin, Alb = albumin, PT-INR = prothrombin time-international normalized ratio, aPTT = activated partial thromboplastin time, AST = aspartate aminotransferase, ALT = alanine aminotransferase, ALP = alkaline phosphatase, GGT = gamma-glutamyl transpeptidase, Cr = creatinine, Na = sodium, PLT = platelet, LPR = liver-to-portal vein signal intensity ratio, LPVC = liver-to-portal vein contrast		

The ICC of measurement of SI among the three readers was 0.92 (95% confidence interval [CI]: 0.89–0.95), indicating a very strong positive correlation between the three readers' measurements. There was substantial to almost perfect agreement (weighted κ = 0.7–0.96) in the pair-wise evaluation and substantial agreement (Fleiss κ = 0.736) among the three readers for classifying parenchymal enhancement grading. The visual assessment showed a significant correlation with quantitative hepatic enhancement with − 0.787 of ρ ($p < 0.001$; Fig. 1).

Correlation between MRI measurements and biochemical parameters.

Table 2 shows the relationships between LPR and the 5-level visual assessment and the biochemical parameters. Decreased serum levels of Alb ($r = 0.518$ for LPR, $p < 0.001$; $\rho = -0.624$ for the 5-level visual assessment, $p < 0.001$), PLT ($r = 0.286$, $p < 0.001$; $\rho = -0.312$, $p < 0.001$), and elevated TB ($r = -0.381$, $p < 0.001$; $\rho = 0.460$, $p < 0.001$), PT-INR ($r = -0.335$, $p < 0.001$; $\rho = 0.442$, $p < 0.001$), CPS ($\rho = -0.482$, $p < 0.001$; $\rho = 0.643$, $p < 0.001$), MELD-Na score ($\rho = -0.427$, $p < 0.001$; $\rho = 0.535$, $p < 0.001$) were significant factors related to decreased hepatic enhancement. Elevated AST ($\rho = 0.311$, $p < 0.001$), ALP ($\rho = 0.166$, $p = 0.015$), GGT ($\rho = 0.241$, $p < 0.001$) and decreased Cr ($\rho = -0.262$, $p < 0.001$) showed a significant relationship with decreased hepatic enhancement only for the 5-level visual assessment.

Table 2

Correlation between biochemical parameters and liver-to-portal vein signal intensity ratio and visual assessment for degree of hepatic enhancement during hepatobiliary phase images.

	Liver-to-portal vein signal intensity ratio		Visual assessment for degree of hepatic enhancement						
			Grade						
	correlation coefficient (r)	p-value†	1 (n = 76)	2 (n = 75)	3 (n = 57)	4 (n = 6)	p-value‡	correlation coefficient (ρ)	p-value§
TB	-0.381	< 0.001	0.8 (0.6, 1)	0.7 (0.5, 1.1)	1.9 (1.15, 2.95)	3.3 (1.78, 4.63)	< 0.001	0.460	< 0.001
Alb	0.518	< 0.001	4.2 (4, 4.5)	3.8 (3.4, 4.2)	3.1 (2.75, 3.45)	2.65 (2.45, 3.25)	< 0.001	-0.624	< 0.001
PT-INR	-0.335	< 0.001	1.08 (1.02, 1.17)	1.11 (1.03, 1.2)	1.27 (1.15, 1.45)	1.42 (1.13, 1.66)	< 0.001	0.442	< 0.001
aPTT	-0.107	0.119	33.1 (30.43, 33.88)	33.1 (29.2, 34.5)	33.1 (30.5, 36.25)	33.4 (30.28,35.05)	0.397	0.089	0.197
AST	0.027	0.693	32 (26.25, 46.75)	37 (28, 65)	51 (37, 83.5)	60 (48, 211.75)	< 0.001	0.311	< 0.001
ALT	0.120	0.081	32 (22, 49.5)	32 (20, 53)	31 (20.5, 46)	22.5 (13.5, 84.5)	0.823	-0.048	0.483
ALP	-0.072	0.298	95.5 (75.25, 128.75)	92 (72, 131)	110 (91.5, 156.5)	115.5 (96.5, 169.75)	0.026	0.166	0.015
GGT	-0.073	0.287	46.5 (30.25, 96.25)	62 (33, 134)	70 (44.5, 170.5)	198.5 (120, 360)	0.002	0.241	< 0.001

Note. - Unless otherwise specified, data are median with interquartile range.

* Data are presented as number (%) of patients.

† P value was calculated by Pearson's correlation coefficient.

‡ P value was calculated by Kruskal-Wallis test.

§ P value was calculated by Spearman's rank correlation coefficient.

	Liver-to-portal vein signal intensity ratio		Visual assessment for degree of hepatic enhancement						
			Grade						
	correlation coefficient (r)	p-value†	1 (n = 76)	2 (n = 75)	3 (n = 57)	4 (n = 6)	p-value‡	correlation coefficient (ρ)	p-value§
Cr	0.004	0.957	0.87 (0.75, 0.99)	0.79 (0.68, 0.97)	0.72 (0.6, 0.91)	0.63 (0.46, 0.73)	0.001	-0.262	< 0.001

Note. - Unless otherwise specified, data are median with interquartile range.

* Data are presented as number (%) of patients.

† P value was calculated by Pearson's correlation coefficient.

‡ P value was calculated by Kruskal-Wallis test.

§ P value was calculated by Spearman's rank correlation coefficient.

	Liver-to-portal vein signal intensity ratio		Visual assessment for degree of hepatic enhancement						
			Grade						
	correlation coefficient (r)	p-value†	1 (n = 76)	2 (n = 75)	3 (n = 57)	4 (n = 6)	p-value‡	correlation coefficient (ρ)	p-value§
Na	0.028	0.679	138 (137, 140)	139 (137, 141)	137 (134.5, 139)	140.5 (136.5, 141.25)	0.008	-0.122	0.076
PLT	0.286	< 0.001	164.5 (100.25, 221.75)	146 (92, 215)	91 (66, 129.5)	82.5 (56.75, 117.25)	< 0.001	-0.312	< 0.001
CPS*	-0.482	< 0.001	5 (5, 6)	6 (5, 7)	7 (7, 8.5)	9 (8, 10.75)	< 0.001	0.643	< 0.001
MELD-Na*	-0.427	< 0.001	8 (7, 9)	8 (7, 10)	13 (10, 17)	14.5 (11, 19.25)	< 0.001	0.535	< 0.001
Note. - Unless otherwise specified, data are median with interquartile range.									
* Data are presented as number (%) of patients.									
† P value was calculated by Pearson's correlation coefficient.									
‡ P value was calculated by Kruskal-Wallis test.									
§ P value was calculated by Spearman's rank correlation coefficient.									

Parameters associated with insufficient liver enhancement

The univariate analysis showed that TB (odds ratio [OR] = 6.027, 95% CI: 3.44–10.55, p < 0.001), Alb (OR = 0.086, 95% CI: 0.04–0.17, p < 0.001), PT-INR (OR = 134.854, 95% CI: 21.64–840.33, p < 0.001), Na (OR = 0.91, 95% CI: 0.84–0.99, p = 0.02), and PLT (OR = 0.99, 95% CI: 0.99–0.99, p < 0.001) were significantly associated with insufficient hepatic enhancement during the HBP imaging (Table 3). The multivariate analysis revealed significant associations with TB (OR = 4.71, 95% CI: 2.2–10.01, p < 0.001) and Alb (OR = 0.12, 95% CI: 0.05–0.29, p < 0.001 [Table 3]).

Table 3
Univariate and multivariate analysis of associated factor of insufficient hepatic enhancement during the hepatobiliary phase images.

	Univariate analysis		Multivariate analysis	
	Odd ratio (95% confidence interval)	p-value	Odd ratio (95% confidence interval)	p-value
TB	6.03 (3.44, 10.55)	< 0.001	4.71 (2.2, 10.01)	< 0.001
Alb	0.086 (0.04, 0.17)	< 0.001	0.12 (0.05, 0.29)	< 0.001
PT-INR	134.85 (21.64, 840.33)	< 0.001	0.2 (0.01, 5.06)	0.325
aPTT	1.02 (0.97, 1.07)	0.465		
AST	1.00 (1, 1.01)	0.100		
ALT	1 (1, 1)	0.865		
ALP	1 (1, 1.01)	0.199		
GGT	1 (1, 1)	0.140		
Cr	1.01 (0.58, 1.76)	0.982		
Na	0.91 (0.84, 0.99)	0.020	1.04 (0.91, 1.19)	0.551
PLT	0.99 (0.99, 0.99)	< 0.001	1 (0.99, 1)	0.529

Diagnostic performance of prediction of insufficient liver enhancement.

Diagnostic performance for the prediction of insufficient liver enhancement based on the KNN algorithm are presented in Table 4 and Fig. 2. The accuracies of the predictive model using KNN were 79.5% for CPS and 80.8% for MELD-Na. The accuracy of the predictive model from a combination of biochemical parameters had a higher accuracy of 82.8% than others (Fig. 3). The AUC of this combination of biochemical parameters showed the highest predictive ability with 0.861, followed by CPS (AUC = 0.845) and MELD-Na (AUC = 0.821). Regarding the 5-level grading of hepatic enhancement, a machine learning model with a KNN algorithm for classification as grade 1 achieved accuracies of 69.8% with CPS, 57.8% with MELD-Na, and 65.2% with a combination of biochemical parameters. For classification as grade 2, the accuracies were 58.6% with CPS, 60.1% with MELD-Na, and 57.7% with a combination of biochemical parameters. The classification accuracies for grade 3 and 4 were 78.0%, and 96.4% with CPS, 78.4%, and 97.0% with MELD-Na, and 80.8%, and 97.3% with a combination of biochemical parameters, respectively (Supplementary Information Table 1).

Table 4
Diagnostic performance of machine learning algorithms for the prediction of insufficient hepatic enhancement during hepatobiliary phase images.

	CPS	MELD-Na	Combination of multiple parameters
Sensitivity, %	95.4 ± 0.03	88.8 ± 0.04	95.6 ± 0.03
Specificity, %	35.6 ± 0.15	62.4 ± 0.07	55.9 ± 0.09
Accuracy, %	79.50 ± 0.06	80.8 ± 0.03	82.8 ± 0.04
AUC	0.85 ± 0.05	0.82 ± 0.06	0.86 ± 0.05
Note. — Data are presented as a mean ± standard deviation.			

Discussion

In this study we showed that laboratory tests reflecting hepatic function are closely related with hepatic enhancement during HBP. Using both quantitative and qualitative assessments, decreased serum levels of Alb, PLT, and elevated TB, PT-INR, CPS, MELD-Na score were related to decreased hepatic enhancement on HBP. Multivariate analyses revealed that increased TB and decreased Alb were significantly associated with decreased hepatic enhancement at HBP. We also used a machine learning algorithm to develop a predictive model for insufficient hepatic enhancement of HBP using a combination of biochemical parameters as well as CPS and MELD-Na, which are well-known scoring systems for reflecting reserved hepatic function. The prediction of insufficient hepatic enhancement during the HBP using KNN with a combination of biochemical parameters showed a higher accuracy and AUC than CPS or MELD-Na.

It would be useful if a simple visual MRI finding could determine the possibility of obscuring focal hepatic lesions due to insufficient enhancement of the background liver parenchyma. Measurements of LPR showed a strong relationship with LPVC grade, which was consistent results with a previous study by Tamada et al. [12]. In this regard, we could easily identify insufficient hepatic enhancement during HBP. Furthermore, our results showed that both measurements of LPR and a 5-level assessment of hepatic enhancement provided similar patterns of association as the biochemical parameters.

Some previous studies have reported the association between liver function and insufficient enhancement during the HBP [9,11]. Biochemical parameters commonly known to be associated with liver function are TB, ALT, ALP, GGT, Alb, PLT, and coagulation tests such as PT-INR [11,16–18]. Our results were consistent with the previous studies. Insufficient hepatic enhancement during HBP was correlated with TB, Alb, PT-INR, platelet, and the 5-level degree of hepatic enhancement during HBP was correlated with TB, Alb, PT-INR, AST, ALP, GGT, Cr, and PLT levels. Multivariate analysis showed that Tb (OR = 4.71) and Alb (OR = 0.12) were the independent factors for predicting insufficient hepatic enhancement on HBP, which showed a stronger correlation than any other single parameter examined. Because GB-EOB-DTPA shares the same transport and excretion pathways as bilirubin, elevated serum TB is thought to reduce hepatocyte uptake and bile secretion of GB-EOB-DTPA [19]. The decrease in serum Alb, which is known as a critical plasma protein produced by the liver, not only reflects the chronicity of liver disease but also has potential diagnostic value for determining a prognosis [20].

As shown in a previous study, many liver function tests and hepatic enhancement have a close relationship with HBP [21,22]. However, because these liver function tests were all different, the combination of these parameters would be a better indicator than a single parameter [17]. Several scoring systems have been accepted for assessment of reserved hepatic function in patients with liver cirrhosis, such as CPS, MELD, and MELD-Na scores [23–25]. In our study, both CPS (r = -0.482, ρ = 0.643) and MELD-Na (r = -0.427, ρ = 0.535) were included among the high correlation factors concerning the LPR and the 5-level visual assessment of hepatic enhancement on HBP.

Machine learning makes it possible to train algorithms to discover and identify complex patterns and relationships within a variety of parameters by semi-automating the extraction of knowledge and insights from complex data. [26] In medicine, predictive studies based on machine learning are emerging and developed algorithms can be directly applied to patient care to improve the accuracy of predicting diseases and subsequent outcomes [27]. Insufficient enhancement during the HBP can cause poor contrast differences between background liver parenchyma and a focal hepatic lesion without uptake of Gd-EOB-DTPA [7,28]. If insufficient enhancement during the HBP can be predicted in advance, image quality can be improved by a delay of the time to obtain the HBP or modification of several sequence parameters such as flip angle and K-space [29,30]. Therefore, it is clinically important to predict insufficient enhancement of liver parenchyma before performing Gd-EOB-DTPA-enhanced MRI. There have been studies to predict insufficient enhancement during the HBP using a traditional classification approach [9,11]. Of our predictive models based on machine learning with the KNN algorithm, the model using a combination of biochemical parameters showed a higher accuracy of 82.8% and AUC of 0.86 than the models using CPS or MELD-Na. As mentioned above, because the various parameters reflecting liver function all work differently, a combination of the various parameters would more accurately determine hepatic enhancement on HBP. While the prediction of insufficient hepatic enhancement on HBP yielded a high diagnostic performance, classification of hepatic enhancement using a 5-level visual assessment showed incomplete results because of the small data set of unbalanced data.

There were some limitations in our study. First, this study was conducted retrospectively, and thus carries the potential for selection bias. Second, the model was developed from a small population in a single center and was not validated using another set of populations. Therefore, our results should be further validated through prospective studies in multiple institutions. Finally, we did not consider the degree of liver fibrosis, which also affects hepatic enhancement on HBP. Liver fibrosis was identified with an invasive biopsy procedure, which has the inherent problems of safety and some degree of sampling error. Nevertheless, research comparing the performance of the predictive models when integrating histopathologic results should be conducted in the future.

In conclusion, radiologists can predict insufficient hepatic enhancement during HBP in advance with a machine learning-based predictive model that uses the KNN algorithm to adjust each patient's individually optimized MRI protocol.

Declarations

Acknowledgments

None

Conflict of interest statement:

The authors declare no conflicts of interest that pertain to this work.

Authors' contributions:

*J.B and S.P contributed equally to this work as co-corresponding authors

J.B and S.P contributed to study concept and design. J.S.K, J.B and J.Y.W acquired, analyzed, interpreted the data. J.B and S.P performed statistical analysis and developed prediction mode. J.S.K and J.B drafted the manuscript. J.S.K, J.B, S.P and J.Y.W made critical revisions to the manuscript.

References

1. Omata, M. *et al.* Asia-Pacific clinical practice guidelines on the management of hepatocellular carcinoma: a 2017 update. *Hepatol Int.* **11**, 317–370 https://doi.org/10.1007/s12072-017-9799-9 (2017).
2. Zizka, J., Klzo, L., Ferda, J., Mrklovský, M. & Bukac, J. Dynamic and delayed contrast enhancement in upper abdominal MRI studies: comparison of gadoxetic acid and gadobutrol. *Eur J Radiol.* **62**, 186–191 https://doi.org/10.1016/j.ejrad.2007.02.035 (2007).
3. Akai, H. *et al.* Fate of hypointense lesions on Gd-EOB-DTPA-enhanced magnetic resonance imaging. *Eur J Radiol.* **81**, 2973–2977 https://doi.org/10.1016/j.ejrad.2012.01.007 (2012).
4. Tsuboyama, T. *et al.* Hepatocellular carcinoma: hepatocyte-selective enhancement at gadoxetic acid-enhanced MR imaging–correlation with expression of sinusoidal and canalicular transporters and bile accumulation. *Radiology.* **255**, 824–833 https://doi.org/10.1148/radiol.10091557 (2010).
5. Kitao, A. *et al.* Hepatocellular carcinoma: signal intensity at gadoxetic acid-enhanced MR Imaging–correlation with molecular transporters and histopathologic features. *Radiology.* **256**, 817–826 https://doi.org/10.1148/radiol.10092214 (2010).
6. Hamm, B. *et al.* Phase I clinical evaluation of Gd-EOB-DTPA as a hepatobiliary MR contrast agent: safety, pharmacokinetics, and MR imaging. *Radiology.* **195**, 785–792 https://doi.org/10.1148/radiology.195.3.7754011 (1995).
7. Verloh, N. *et al.* Impact of liver cirrhosis on liver enhancement at Gd-EOB-DTPA enhanced MRI at 3 Tesla. *Eur J Radiol.* **82**, 1710–1715 https://doi.org/10.1016/j.ejrad.2013.05.033 (2013).
8. Tajima, T. *et al.* Relationship between liver function and liver signal intensity in hepatobiliary phase of gadolinium ethoxybenzyl diethylenetriamine pentaacetic acid-enhanced magnetic resonance imaging. *J Comput Assist Tomogr.* **34**, 362–366 https://doi.org/10.1097/RCT.0b013e3181cd3304 (2010).
9. Motosugi, U. *et al.* Liver parenchymal enhancement of hepatocyte-phase images in Gd-EOB-DTPA-enhanced MR imaging: which biological markers of the liver function affect the enhancement? *J Magn Reson Imaging.* **30**, 1042–1046 https://doi.org/10.1002/jmri.21956 (2009).
10. Kim, A. Y. *et al.* Detection of hepatocellular carcinoma in gadoxetic acid-enhanced MRI and diffusion-weighted MRI with respect to the severity of liver cirrhosis. *Acta Radiol.* **53**, 830–838 https://doi.org/10.1258/ar.2012.120099 (2012).
11. Cui, E. *et al.* Development and validation of a predictor of insufficient enhancement during the hepatobiliary phase of Gd-EOB-DTPA-enhanced magnetic resonance imaging. *Acta Radiol.* **58**, 1174–1181 https://doi.org/10.1177/0284185116687170 (2017).

12. Tamada, T. *et al.* Simple Method for evaluating the degree of liver parenchymal enhancement in the hepatobiliary phase of gadoxetic acid-enhanced magnetic resonance imaging. *J Magn Reson Imaging.* **37**, 1115–1121 https://doi.org/10.1002/jmri.23912 (2013).
13. Kamath, P. S. *et al.* A model to predict survival in patients with end-stage liver disease. *Hepatology.* **33**, 464–470 https://doi.org/10.1053/jhep.2001.22172 (2001).
14. Kim, W. R. *et al.* Hyponatremia and mortality among patients on the liver-transplant waiting list. *N Engl J Med.* **359**, 1018–1026 https://doi.org/10.1056/NEJMoa0801209 (2008).
15. Landis, J. R. & Koch, G. G. The measurement of observer agreement for categorical data. *Biometrics.* **33**, 159–174 (1977).
16. Higaki, A. *et al.* Potential clinical factors affecting hepatobiliary enhancement at Gd-EOB-DTPA-enhanced MR imaging. *Magn Reson Imaging.* **30**, 689–693 https://doi.org/10.1016/j.mri.2012.01.004 (2012).
17. Mori, Y. *et al.* Predicting Patients With Insufficient Liver Enhancement in the Hepatobiliary Phase Before the Injection of Gadoxetic Acid: A Practical Approach Using the Bayesian Method. *J Magn Reson Imaging.* **51**, 62–69 https://doi.org/10.1002/jmri.26760 (2020).
18. Sakka, S. G. Assessing liver function. *Curr Opin Crit Care.* **13**, 207–214 https://doi.org/10.1097/MCC.0b013e328012b268 (2007).
19. Hagenbuch, B. & Gui, C. Xenobiotic transporters of the human organic anion transporting polypeptides (OATP) family. *Xenobiotica.* **38**, 778–801 https://doi.org/10.1080/00498250801986951 (2008).
20. Spinella, R., Sawhney, R. & Jalan, R. Albumin in chronic liver disease: structure, functions and therapeutic implications. *Hepatol Int.* **10**, 124–132 https://doi.org/10.1007/s12072-015-9665-6 (2016).
21. Yamada, A. *et al.* Quantitative evaluation of liver function with use of gadoxetate disodium-enhanced MR imaging. *Radiology.* **260**, 727–733 https://doi.org/10.1148/radiol.11100586 (2011).
22. Chen, B. B. *et al.* Dynamic contrast-enhanced magnetic resonance imaging with Gd-EOB-DTPA for the evaluation of liver fibrosis in chronic hepatitis patients. *Eur Radiol.* **22**, 171–180 https://doi.org/10.1007/s00330-011-2249-5 (2012).
23. Botta, F. *et al.* MELD scoring system is useful for predicting prognosis in patients with liver cirrhosis and is correlated with residual liver function: a European study. *Gut.* **52**, 134–139 https://doi.org/10.1136/gut.52.1.134 (2003).
24. Durand, F. & Valla, D. Assessment of the prognosis of cirrhosis: Child-Pugh versus MELD. *J Hepatol.* **42 Suppl**, S100–107 https://doi.org/10.1016/j.jhep.2004.11.015 (2005).
25. Kim, K. M. *et al.* Child-Pugh, MELD, MELD-Na, and ALBI scores: which liver function models best predicts prognosis for HCC patient with ascites? *Scand J Gastroenterol.* **55**, 951–957 https://doi.org/10.1080/00365521.2020.1788139 (2020).
26. Najafabadi, M. M. *et al.* Deep learning applications and challenges in big data analytics. *Journal of Big Data.* **2**, 1 https://doi.org/10.1186/s40537-014-0007-7 (2015).
27. Wong, N. C., Lam, C., Patterson, L. & Shayegan, B. Use of machine learning to predict early biochemical recurrence after robot-assisted prostatectomy. *BJU Int.* **123**, 51–57 https://doi.org/10.1111/bju.14477 (2019).
28. Verloh, N. *et al.* Assessing liver function by liver enhancement during the hepatobiliary phase with Gd-EOB-DTPA-enhanced MRI at 3 Tesla. *Eur Radiol.* **24**, 1013–1019 https://doi.org/10.1007/s00330-014-3108-y (2014).

29. Esterson, Y. B. *et al.* Improved parenchymal liver enhancement with extended delay on Gd-EOB-DTPA-enhanced MRI in patients with parenchymal liver disease: associated clinical and imaging factors. *Clin Radiol.* **70**, 723–729 https://doi.org/10.1016/j.crad.2015.03.005 (2015).
30. Rosenkrantz, A. B., Block, T. K., Hindman, N., Vega, E. & Chandarana, H. Combination of increased flip angle, radial k-space trajectory, and free breathing acquisition for improved detection of a biliary variant at living donor liver transplant evaluation using gadoxetic acid-enhanced MRCP. *J Comput Assist Tomogr.* **38**, 277–280 https://doi.org/10.1097/rct.0000000000000071 (2014).

Figures

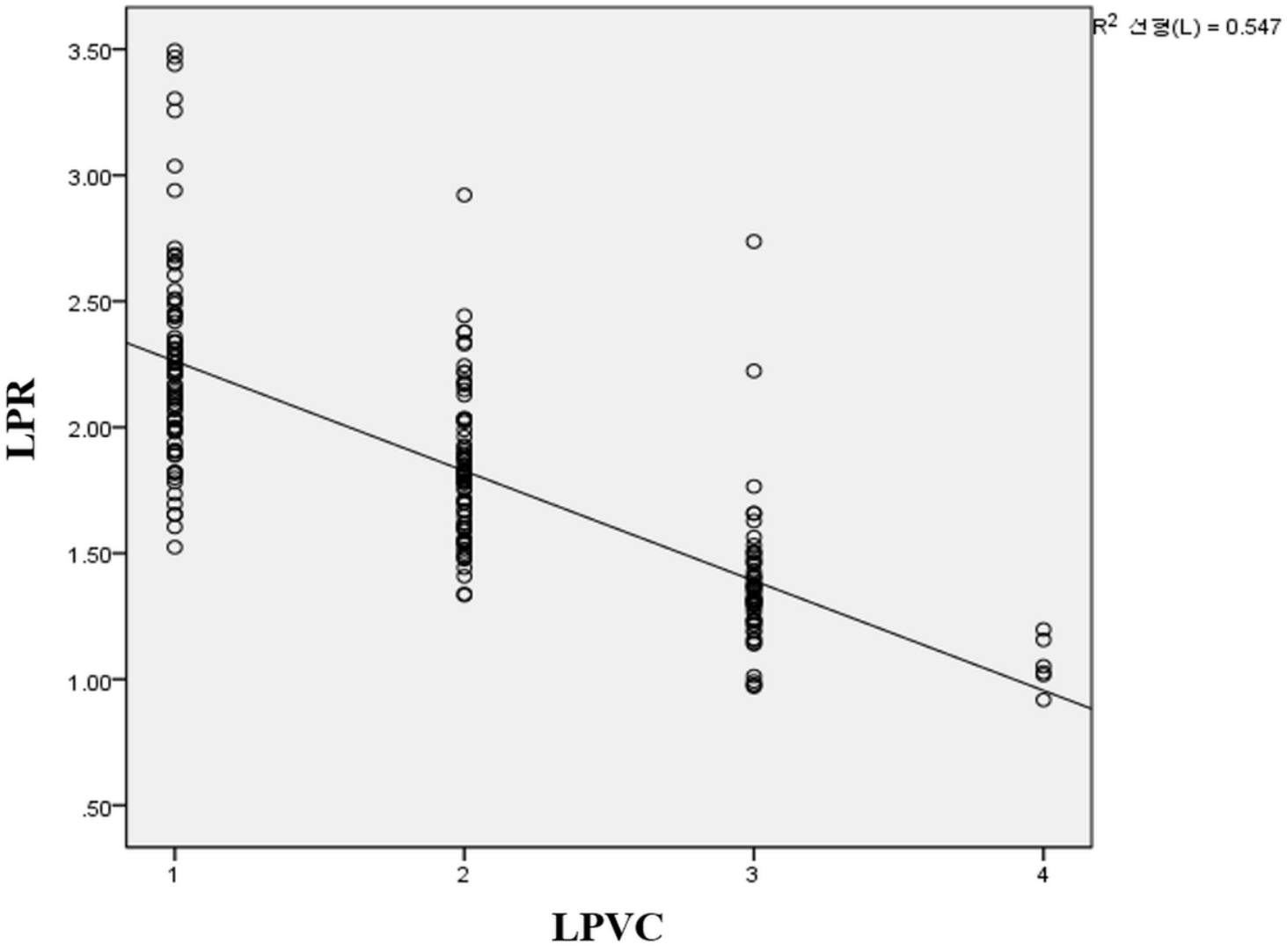

Figure 1

Scatterplots showing relationship between LPR and LPVC LPR = liver-to-portal vein signal intensity ratio; LPVC = liver-to-portal vein contrast

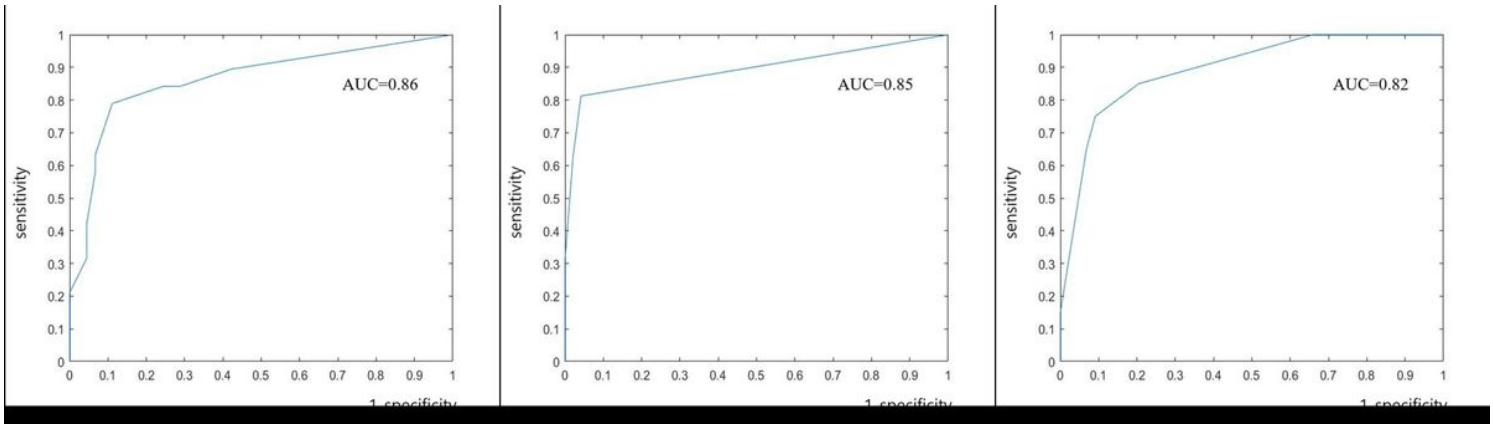

Figure 2

Receiver operating characteristic curve for prediction model of insufficient hepatic enhancement during HBP for combination of various parameters (left panel -a; AUC=0.86), CPS (Middle panel-b; AUC=0.85), and MELD-Na (Right panel-c; AUC=0.82)

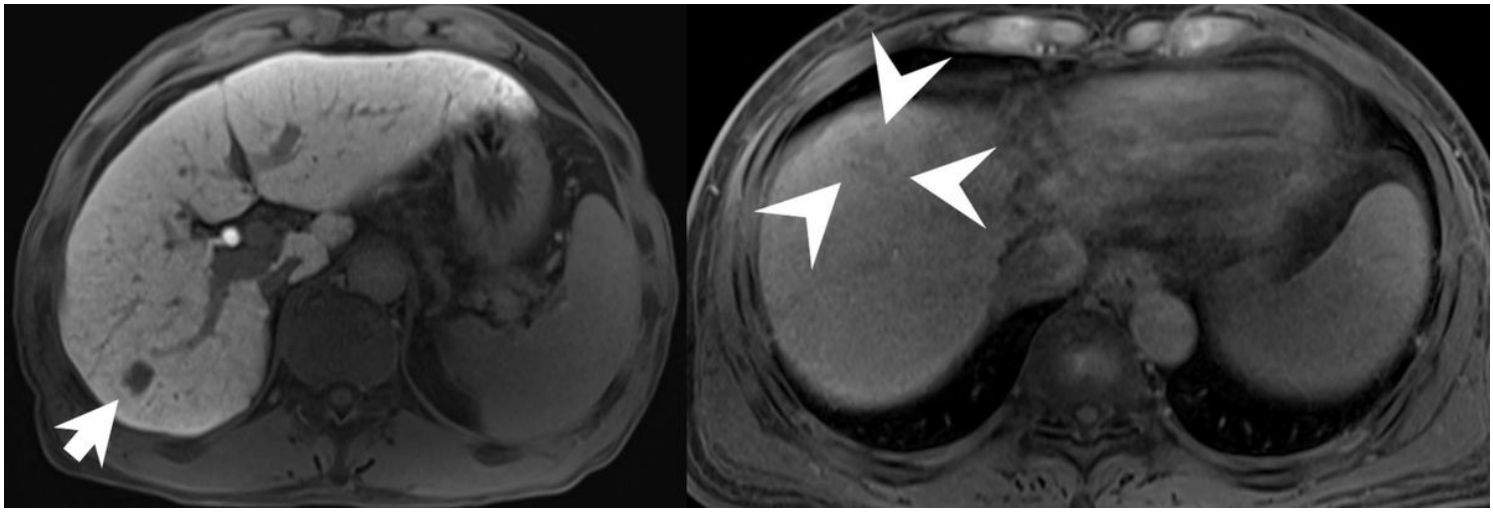

Figure 3

Association between liver function and insufficient enhancement during the HBP. HBP images of Gd-EOB-DTPA MRI of a 22-year-old male patient (Left panel-a) shows definite defect nodule (arrow, confirmed as HCC) showing high conspicuity. Calculated LPR was 2.28 and visual assessment was classified as grade 1. His all liver function test shows within normal range. HBP images of Gd-EOB-DTPA MRI of a 58-year-old male patient (Right panel-b) shows subtle defect lesion (arrowheads, confirmed as HCC). Calculated LPR was 1.35 and visual assessment was classified as grade 4. In laboratory test, increased level of TB (6 mg/dL) and decreased level of Alb (3 g/dL) was confirmed. CPS was 8 and MELD-Na was 16.

Supplementary Files

This is a list of supplementary files associated with this preprint. Click to download.

- HBPsupplementarySR.docx